Title

Tunable sustained intravitreal drug delivery system for daunorubicin using oxidized porous silicon

Journal

Journal of Controlled Release, 178(1)

ISSN

0168-3659

Authors

Hou, Huiyuan
Nieto, Alejandra
Ma, Feiyan
et al.

Publication Date

2014-03-01

DOI

10.1016/j.jconrel.2014.01.003

Peer reviewed

Published in final edited form as:
J Control Release. 2014 March 28; 178: 46–54. doi:10.1016/j.jconrel.2014.01.003.

Tunable sustained intravitreal drug delivery system for daunorubicin using oxidized porous silicon

Huiyuan Hou[1,2,†], **Alejandra Nieto**[1,2,†], **Feiyan Ma**[1], **William R. Freeman**[1], **Michael J. Sailor**[2], and **Lingyun Cheng**[1]

[1]Department of Ophthalmology, Jacobs Retina Center at Shiley Eye Center, University of California San Diego, La Jolla, CA

[2]Department of Chemistry and Biochemistry, University of California San Diego, La Jolla, CA

Abstract

Daunorubicin (DNR) is an effective inhibitor of an array of proteins involved in neovascularization, including VEGF and PDGF. These growth factors are directly related to retina scar formation in many devastating retinal diseases. Due to the short vitreous half-life and narrow therapeutic window, ocular application of DNR is limited. It has been shown that a porous silicon (pSi) based delivery system can extend DNR vitreous residence from a few days to 3 months. In this study we investigated the feasibility of altering the pore size of the silicon particles to regulate the payload release. Modulation of the etching parameters allowed control of the nano-pore size from 15 nm to 95 nm. In vitro studies showed that degradation of pSi O_2 increased with increasing pore size and the degradation of pSi O_2 was approximately constant for a given particle type. The degradation of pSi O_2 with 43 nm pores was significantly greater than the other two particles with smaller pores, judged by observed and normalized mean Si concentration of the dissolution samples (44.2±8.9 vs 25.7±5.6 or 21.2±4.2 μg/mL, $p<0.0001$). In vitro dynamic DNR release revealed that $pSiO_2$-CO_2H:DNR (Porous silicon dioxide with covalent loading of daunorubicin) with large pores (43 nm) yielded a significantly higher DNR level than particles with 15 or 26 nm pores (13.5±6.9 ng/mL vs. 2.3±1.6 ng/mL and 1.1±0.9 ng/mL, $p<0.0001$). After two months of in vitro dynamic release, 54% of the $pSiO_2$-CO_2H:DNR particles still remained in the dissolution chamber by weight. In vivo drug release study demonstrated that free DNR in vitreous at post-injection day 14 was 66.52 ng/mL for 95 nm pore size $pSiO_2$-CO_2H:DNR, 10.76 ng/mL for 43 nm pSi O_2-CO_2 H:DNR, and only 1.05 ng/mL for 15 nm pSi O_2-CO_2 H:DNR. Pore expansion from 15 nm to 95 nm led to a 63 folds increase of DNR release ($p<0.0001$) and a direct correlation between the pore size and the drug levels in the living eye vitreous was confirmed. The present study demonstrates the feasibility of regulating DNR release from pSi O_2 covalently loaded with DNR by engineering the nano-pore size of pSi.

Correspondence to: Lingyun Cheng, MD, Department of Ophthalmology, Jacobs Retina Center at Shiley Eye Center, University of California, San Diego, 9415 Campus Point Drive, La Jolla, CA 92093-0946. Tel: 858-534-3780; Fax:858-534-7985; cheng@eyecenter.ucsd.edu.
[†]Both authors contributed equally to this work

Disclosure: W.R. Freeman, Spinnaker Biosciences (C); M.J. Sailor, Spinnaker Biosciences (I); L. Cheng, Spinnaker Biosciences (C)

Chemical compounds studied in the article:
Silicon; Silicon Dioxide; Daunorubicin Hydrochloride; Hydrofluoric Acid; Ethanol; 3-aminopropyltrimethoxysilane; Succinic Anhydride; N,N-dimethylformamide; N-(3-dimethylaminopropyl)-N´-ethylcarbodiimide hydrochloride; Nitrogen

Keywords

Porous silicon; Controlled drug release; Intravitreal drug delivery; Daunorubicin; Rabbit eye

Introduction

Proliferative vitreoretinopathy (PVR) is the major vision threatening complication for rhegmatogenous retinal detachment. Proliferation of endongenous retinal cells, such as retinal pigment epithelium (RPE) and glial cells, as well as visiting immune cells at the vitreoretinal interface leads to the formation of vitreoretinal membranes which cause tractional retinal detachment and vision loss.[1] Inhibition of proliferation of these cells by chemotherapeutic agents has been the primary target of PVR prevention.[2],[3] Daunorubicin (DNR) is one of the potential therapeutic agents for unwanted ocular proliferation. It has been shown to be effective for treatment of PVR on animal models and in clinical studies.[4–7] However, the short intravitreal half-life and narrow therapeutic window of DNR,[8] which implies frequent intravitreal injections over time to obtain sustained treatment, hinder its further clinical application. An optimal ocular drug delivery system, which could provide a sustained and long-lasting presence of DNR at the disease site, would bean ideal solution. For this purpose we have proposed porous silicon (pSi) as a biodegradable carrier for intravitreal drug delivery.[9–11] The nanostructure of pSi provides reservoirs which host therapeutics and provide sustained drug release after a single intravitreal injection. We have demonstrated that intravitreal pSi injection is safe in rabbit eyes.[9] It degrades to completely soluble and excretable orthosilicates.[12] DNR can be covalently loaded into pSi for sustained intravitreal drug delivery as the carrier degrades.[10] We hypothesize that the rate of drug release, as well as the ocular therapeutic duration may be controllable by altering the nano-pore size of the pSi. Previous work has shown that the rate of degradation of pSi in aqueous media can be dependent on pore size and surface morphology.[13] Most recently, Martinez et al demonstrated in vitro a positive correlation between pore size and degradation rate of oxidized and 3-aminopropyl triethoxysilane functionalized pSi particles in phosphate buffered saline. However, subsequent quantum dot infiltration loading and release showed the release rate was negatively associated with the pore size of the pSi particles.[14] In the current study, we investigated the influence and capacity of changing pore size of $pSiO_2$ microparticles on the rate of drug release using DNR as a model drug. We are interested in knowing if the relationship between pore size and pSi degradation would translate into a similar relationship between pore size and daunorubicin release if we use a covalent drug loading strategy instead of infiltration loading which released daunorubicin too fast and caused retinal toxicity.[10] We are also interested in knowing the capacity of this tenability in a living eye to gauge the feasibility of this intravitreal drug delivery system to prevent and treat PVR.

Material and Methods

Synthesis of pSi microparticles

pSi microparticles were prepared by anodic electrochemical etch of highly doped, (100)-oriented, p-type silicon wafers (Siltronix Inc., Archamps, France, boron-doped, 1.00 ±0.01 mΩ·cm resistivity), as previously described.[10, 15] A silicon wafer with an exposed area of 8.04 cm^2 was contacted on the backside with a strip of aluminum foil and mounted in a Teflon etching cell that was fitted with a platinum counter-electrode. The etching conditions to obtain pSi microparticles with different pore sizes, including current density and etch duration, are summarized in Table 1. Particles A and B were etched in a 3:1 (v/v) solution of 48% aqueous hydrofluoric acid (HF) and absolute ethanol (Fisher-Scientific, Pittsburg, PA).

Particles C and D were etched in a 1:1 (v/v) solution of 48% aqueous HF and absolute ethanol. The wafers were etched at a constant current density (mA/cm^2), and the porous layer resulting from every etch was removed from the silicon substrate by electro polishing in a 1:29 solution of 48% aqueous HF and absolute ethanol for 120 seconds (Table 1). The etching and electro polishing procedure was repeated 20 times per wafer. The films were harvested every 4 etches and the resulting porous layers were ultrasonicatedin ethanol (FS5 dual action ultrasonic cleaner, Thermo Fisher Scientific, Pittsburg, PA) for 30 minutes to form the pSi particles. After ultrasonic treatment, the supernatant was removed and the particles were resuspended in ethanol. This procedure was repeated a total of three times until the supernatant was transparent. The pSi particles were isolated, dried at room temperature and stored under vacuum in a desiccator.

DNR loading into porous silica ($pSiO_2$) microparticles

DNR was loaded into particles A, C and D by covalent attachment by creating a chemical bond between the drug and functional groups placed on the particle surface, as previously described.[10] Briefly, pSi particles were placed in a ceramic boat, heated from room temperature to 800 °C inside a muffle furnace (Thermo Fisher Scientific, Pittsburg, PA), and maintained at 800 °C for 1 hour in order to fully oxidize pSi to $pSiO_2$. The samples were removed from the chamber after the furnace had cooled to room temperature. The resulting $pSiO_2$ particles were then treated with an aqueous HCl solution (2% concentrated HCl by volume) for 1 hour, rinsed three times with water and dried. The particles were then vortexedin a 1% 3-aminopropyltrimethoxysilane (Sigma-Aldrich) in ethanol solution for 1 hour, rinsed with ethanol, and dried, resulting in alkylamine-modified particles. The amine-functionalized porous SiO_2 particles were reacted with 0.1 M succinic anhydride (99%, Sigma-Aldrich) in N,N-dimethylformamide (DMF, Sigma-Aldrich) for 16 hours and rinsed with water to obtain a carboxylic acid functional surface ($pSiO_2$-CO_2H). The carboxylic acid group resulted from the ring opening of succinic anhydride through reaction with the amine group on the surface of the particles.[10, 16] The surface carboxyl species were then activated by treatment with an aqueous solution containing 68 mM N-(3-dimethylaminopropyl)-N´-ethylcarbodiimide hydrochloride (EDC, Sigma-Aldrich; 8.45 mg) and 6.5 mM N-hydroxysulfosuccinimide (Sulfo-NHS, Pierce Biotechnology Inc, Rockford, IL; 0.92 mg). The coupling reagents were added to a dispersion of $pSiO_2$-CO_2H particles in aqueous phosphate buffered saline (PBS, pH 7.4, Fisher Scientific) containing 10% dimethyl sulfoxide by volume (DMSO, Alfa Aesar, Ward Hill, MA). DNR was then coupled to the activated surface by addition of an aqueous solution (200 μL) containing 1 mg/mL daunorubicin hydrochloride (Tocris Biosciences, Bristol, UK) to the particle mixture, as previously described.[10] After the loading procedure, the particles were pelletized by centrifugation and carefully rinsed with ethanol five times until the washing solution was close to transparent in order to remove unloaded drug and any excess cross linkers. At this point, the particles were observed to have changed from an initial white translucent appearance to the deep orange color of DNR. Average particle size and pore size of the $pSiO_2$ particles were determined from scanning electron microscope (SEM) plan-view images from randomly selected particles (n>5) using a Phillips XL30 field emission electron microscope operating at an accelerating voltage of 5 kV (FEI Phillips, Hillsboro, OR).[10, 17] The particle thickness and open porosity were calculated by optical measurements of the reflectivity spectrum as a function of liquid infiltration using the spectroscopy liquid infiltration method (SLIM).[18] The textural properties of the $pSiO_2$ particles were analyzed by nitrogen sorption at −196 °C on an ASAP 2020 porosimetry apparatus (Micromeritics, Norcross, GA). Prior to the sorption experiment, approximately 50 mg of the porous silicon sample was out gassed overnight at 105 °C. The specific surface area (m^2/g) and pore volume (cm^3/g) of the particles were calculated from the N_2 adsorption/desorption isotherms

by using the BET (Brunauer-Emmett-Teller) and BJH (Barrett-Joyner-Halenda) methods, respectively.[19–21]

The presence of the functional linker on the $pSiO_2$-CO_2H surface as well as the successful covalent attachment of DNR to the microparticles was confirmed by attenuated total reflectance Fourier transform infrared (ATR-FTIR) spectroscopy using a Nicolet 6700 FT-IR spectrometer with Smart-ATR attachment (Nicolet Instruments Inc., Madison, WI). Drug loading efficiency of each type of particle ($pSiO_2$-CO_2H:DNR) was analyzed by thermogravimetry (TGA). The DNR-loaded samples (~2 mg) were placed in a 90 μL alumina sample cup. Samples were heated at a constant rate of 10 °C/minute up to 800 °C in nitrogen atmosphere with a purge rate of 10 mL/min using a Q600 simultaneous TGA/DSC apparatus (TA Instruments, New Castle, DE). Weight percent loading efficiency of DNR in the samples was determined by analyzing TGA curves of $pSiO_2$-CO_2H ($pSiO_2$ with carboxylic acid functional surface) as well as $pSiO_2$-CO_2H:DNR ($pSiO_2$ containing DNR covalently attached to the pore walls), as shown previously.[10],[11]

In vitro degradation test of empty $pSiO_2$ particles with different pore sizes

The effect of the different textural characteristics of the $pSiO_2$ particles on in vitro degradation behavior was examined by immersing particles A, B and C (Table 1) in 1.5 mL Hank's Balanced Salt Solution (HBSS, Cellgro, Mediatech Inc, Manassas, VA) at 37 °C over a period of 32 days. The entire supernatant (1.3 ml) was collected at the same time every day after centrifugation at 13,000 rpm for 10 min and stored at −80 °C until analysis. At each sampling time-point (day), an equal volume (1.3 mL) of fresh buffer was added back into the vial to restore the sink conditions. The silicon concentration of the samples was quantitated by Inductively Coupled Plasma-Optical Emission Spectroscopy (ICP-OES).

In vitro drug release study

Dynamic drug release was simulated in vitro using a custom-designed flow chamber and a syringe pump. The particles were weighed into an eppendorf tube and suspended in 100 μL HBSS immediately before injection into the flow chamber using the same syringe and needle as for an intravitreal application. The flow chamber circulation volume was 1.5 mL to mimic the rabbit vitreous.[22] An estimated 3 mg of particles A, C, or D was injected in to three different flow chambers. Each chamber was pumped by a NE-1000 syringe pump (New Era Pump Systems, Farmingdale, NY) with a constant flow rate of 1 μL/min using HBSS. From the in vitro degradation study, the degradation rates of the $pSiO_2$ samples containing 15 and 26 nm-diameter pores were comparable. Therefore we used the particles A, C, and D for in vitro and in vivo drug release study. The entire setup was maintained at 37 °C. After the particles had been injected into the chamber, the particles remaining in the eppendorf tube, syringe and needle were carefully collected, rinsed with deionized water, dried under vacuum, and weighed to calculate the actual dose injected. During the 60 days' release, the infusate was collected at the same time every day. The samples were stored at −80 °C until HPLC/MS/MS analysis. The chromatographic separation was performed on a Shiseido Cap cell Pak MG III C-18 column (2.0 mm ID × 50 mm length, 3 μm) with a guard column. Mobile phase A was 2.5% by volume methanol (CH_3OH, Sigma Aldrich, HPLC-grade) in water with 0.1% formic acid (HCOOH, Sigma-Aldrich). Pure methanol with 0.1% by volume formic acid was used as mobile phase B. The mobile phase was delivered at a rate of 200 μL/min under gradient conditions as follows: 30% phase B to 95% phase B in 10 minutes, followed by 6 minutes with 95% phase B and then back to 30% phase B in 1 minute. An additional time of 8 minutes at 30% phase B was used to equilibrate the column and return the system to the initial conditions for subsequent analysis. The LC-ESI-MS/MS was operated under selected reaction monitoring (SRM) scan mode to detect DNR and the

spiked internal standard doxorubicin (DOX, Fisher Bioreagents Inc, Pittsburg, PA). A LC-ESI-MS/MS run of pure HBSS was used as a blank control.

In vivo ocular drug release study

Twelve New Zealand Red rabbits were divided into three groups and used to study the intraocular safety and drug release properties of the three types (A, C, D) of $pSiO_2$-CO_2H:DNR particles. Three rabbits were used as control. All animal studies were performed according to the ARVO statement for the Use of Animals in Ophthalmic and Vision Research, and were approved by The Institutional Animal Care and Use Committee of University of California, San Diego. Only one eye of each animal was used for $pSiO_2$-CO_2H:DNR intravitreal injection. For the intravitreal injection procedure, the rabbits were anesthetized with intramuscular injections of 20 mg/kg ketamine (Fort Dodge Animal Health, Fort Dodge, IA) and 5 mg/kg xylazine (Akorn Inc., Decatur, IL). Slit lamp and indirect ophthalmoscopy were performed on all animal eyes before injection. Baseline fund us images were recorded with a Canon film camera (Canon F-A; Canon Inc., Japan). After disinfecting the eye, 3 mg of $pSiO_2$-CO_2H:DNR particles suspended in 100 μL sterile balanced salt solution (BSS) was injected into the midvitreous cavity of the right eye under direct view of a surgical microscope. The control rabbits were injected with 5 μg free DNR in 50 μL BSS into the right eye. All injections were done using a 1-mL syringe and 27-gauge needle. The eyes were examined at day 1, 3, 7 and 14 after injection using slit lamp biomicroscopy, a handheld tonometer (Tonopen; Medtronic, Jacksonville, FL) for IOP, and indirect ophthalmoscopy. Color fund us photographs were taken at each exam. All rabbits were sacrificed at day 14. After sacrifice, eye globes were enucleated and dissected. After cornea and lens were removed, vitreous was sampled using a 3-mL syringe as we described previously.[23] Whole vitreous was centrifuged for 20 min at 5,000 rpm, and vitreous supernatant was subjected to HPLC/MS/MS ((An Agilent (Santa Clara, CA) 1260 HPLC system coupled with a Thermo (Waltham, MA) LCQ^{deca} mass spectrometer)) analysis using positive ion mode electro spray ionization (ESI) as we described previously.[10, 11]

Cell proliferation assay on rabbit vitreous supernatant

The biological effect of DNR released from particles D in the rabbit vitreous was tested on a human RPE cell line (ARPE-19 cells) using the cell proliferation assay (WST-1) as per the manufacturer's instructions (Roche Diagnostics Corp., Indianapolis, IN). Briefly, the ARPE-19 cells were seeded at a density of 10,000 cells/well into a 96-well plate with DMEM/F-12 medium containing 10% (by volume) FBS and incubated at 37 °C 5% CO_2 for 24 hours to allow the cells to attach. The cell medium was replaced with a mixture of 75% (by volume) culture medium and 25% (by volume) of the supernatant of the vitreous samples from the eyes injected with 3 mg $pSiO_2$-CO_2H:DNR particles with 95 nm pore size. After 5 days of incubation at 37 °C and 5% CO_2, 10 μL WST-1 reagent was added and incubated at 37 °C and 5% CO_2 for 2 hours. The optical density of the developed color was measured at 440 nm. The optical density (OD) was compared with positive controls and negative controls which were cultured in equivalent conditions.

Statistical analysis

For in vitro and in vivo drug release, the data was normalized using the initial drug loading dose. For the in vivo study, IOP was recorded multiple times at different time points from both eyes, hence paired *t* test was used. Drug levels of in vitro and in vivo samples from the different groups and different time points were compared using nonparametric statistical method due to the small sample size. All analyses were performed using JMP statistical software (version 10; SAS Institute Inc, Cary, NC) and a p-value smaller than 0.05 was considered to be significant.

Results

Characterization of the particle texture

SEM measurements revealed that pore size and porosity increased from particle A to particle D (Figure 1). Average particle size, pore size and porosity values for each type of particle are summarized in Table 2.

The specific surface area (S_{BET}), pore size diameter (D_p) and total pore volume (V_T) parameters calculated from the N_2 adsorption/desorption isotherms of particles A-Dare shown in Table 2. The isotherms exhibited classical type IV hysteresis loops with parallel adsorption and desorption branches suggesting cylindrical mesopores of approximately constant cross section. As an example, the N_2 adsorption/desorption isotherms of $pSiO_2$ particle A are shown in Figure 2. The pore size calculated from the adsorption branch of the isotherms was consistent with the pore size calculated from SEM images, with the exception of particle D, where the pore size (95 nm as determined by SEM) was beyond the detection limit for this sorption technique (valid in the pore size range 2–50 nm). Finally, an increase in the total pore volume (V_T) and a decrease in specific surface area (S_{BET}) were observed along with pore size increase. Whereas the increase in total pore volume correlates well with an increase in open porosity and a pore size expansion, we hypothesize the decrease in surface area might be due by a decrease in pore wall thickness or a decrease in the roughness of the inner pore surface, as pores are expanded.

Drug loading by covalent attachment and pore size

DNR covalent attachment to microparticles was confirmed by FTIR. Characteristic vibrational bands were observed at ~1719 cm^{-1} (ν C=O), ~1640 cm^{-1} (amide I), and ~1556 cm^{-1} (amide II) (results not shown). The shift in the characteristic vibrational bands associated with amide bonds before and after DNR grafting provided evidence of successful drug loading by covalent attachment [10]. The DNR loading efficiency in $pSiO_2$-CO_2H:DNR particles A, C, and D as calculated by TGA is shown in Table 2. The drug loading efficiency ranged 7 – 8% by weight.

In vitro $pSiO_2$ degradation and pore size

The rate of $pSiO_2$ particle degradation was found to be well correlated with particle pore size. As expected, among particles of similar sizes, those particles with larger pores were found to degrade faster. The mean Si concentration detected in solution after 32-day degradation of the 43 nm pore size particle (C) was significantly higher than that of the other two particles (B and A), respectively (44.2 vs 25.7 and 21.2 μg/mL, $p<0.0001$, ANOVA) (Figure 3).

In vitro DNR release from the $pSiO_2$-CO_2H:DNR microparticles with different pore size

As observed during the $pSiO_2$ in vitro degradation study, the observed differences in degradation rate of $pSiO_2$ particles with pore size 15 nm (A) and 26 nm (B) were not significant. Therefore, particles A, C, and D (Table 1) were used for the in vitro as well as for the in vivo drug release studies. After a 60 day in vitro release, particle type D demonstrated a 46% decrease by weight, indicative of a decrease in the amount of $pSiO_2$ microparticles in the dissolution chamber over time (Figure 4).

The $pSiO_2$-CO_2H:DNR particles with the largest pore size (95 nm, particle type D) demonstrated a significantly larger quantity of observed and normalized mean DNR release (13.5±6.9 ng/mL) in vitro relative to the other two $pSiO_2$-CO_2H:DNR particle types with smaller pores (2.3±1.6 ng/mL and 1.1±0.9 ng/mL, Figure 5, $p<0.0001$, ANOVA). There was no significant difference in the quantity of DNR released for the $pSiO_2$-CO_2H:DNR

particles with smaller pores (15 nm vs. 43 nm, particle types A and C, respectively, p=0.84, t test).

In vivo ocular drug release from $pSiO_2$-CO_2H:DNR particles with different pores

DNR levels in rabbit vitreous at week two following intravitreal injection of particle types A, C, and D showed a close positive association with the pore sizes. The absolute mean DNR concentration in the rabbit eye over the two-week period was 1.05±0.78 ng/mL for 15 nm pore size particle, while 10.76±4.45 ng/mL and 66.52±12.38 ng/mL for 43 nm and 95 nm pore size particles, respectively. With the equivalent dosing of drug (dose normalization), higher levels of DNR in the rabbit vitreous were found using particles with larger pore sizes. The pore size was significantly associated with the drug levels in the vitreous with both regression analyses but the quadratic analysis fit better and provided a higher R Square (R Square=0.95 vs. R Square=0.92; p value for pore size is <0.0001 for both analysis).

During 2 weeks of clinical observation, the injected particles did not show a noticeable change in the vitreous and no signs of toxicity were observed (Figure 7). Compared to the non-injected fellow eyes, the injected eyes showed similar IOP before sacrifice. For 15 nm pore $pSiO_2$-CO_2H:DNR particles (Type A), IOP of the right eye was 10.4 vs. 9.7 mmHg for the left eye (p=0.34 paired t test); for 43 nm pore particles (Type C), IOP of the right eye was 10.1 vs. 10.7 mmHg for the left eye (p=0.23 paired t test); and for the 95 nm pore particles (Type D), IOP of right eye was 11.35 vs. 10.25 mmHg for left eye (p=0.15 paired t test, Figure 8).

Confirmation of biological effect of the released DNR on cell proliferation assay

Vitreous supernatants from particle D showed significant inhibitory effect in proliferation assays using ARPE-19 cells compared with untreated vitreous. In these experiments, 100 uL of vitreous was introduced to the cell culture. The extent of inhibition of 100 uL of vitreous obtained from a rabbit eye 2 weeks post injection with 3 mg of particle type D was equivalent to a positive control consisting of 100 uL of vitreous spiked with 4.8 ng of DNR (Figure 9, Table 3).

Discussion

DNR is an anthracycline drug that inhibits cell proliferation and migration. The use of this drug has been found to improve the surgical results for PVR and reduce the risk of reoperation for PVR patients.[24, 25] However, after an intravitreal bolus injection of free DNR, the drug level in vitreous quickly drops below the therapeutic level. Previous work has shown that the half-life of DNR in vitreous is very short, only 131 minutes. Therapeutic concentrations of the drug can be maintained for only 4 hours after injection.[8] DNR has a narrow therapeutic window following a single intravitreal injection,[26, 27] which makes the sustained critical level even more difficult to achieve.[8] Although subdivided administrations of a given dose of DNR have been shown to be more effective in preventing experimental PVR than a single dose of the same quantity of drug,[5] the clinical application of DNR against PVR is a significant challenge without a sustained drug delivery system. The current study is aimed at exploring a sustained and controllable delivery system for DNR.

Porous Si exhibits a number of properties that make it an attractive material for controlled drug delivery in the eye. We previously demonstrated good intravitreal biocompatibility of pSi microparticles[9] and we have recently shown the feasibility of a pSi platform for the sustained delivery of DNR.[10] The current study demonstrates the tunability of this

delivery system for the release of a predetermined dose of a drug payload. This is a very important feature for a successful ocular drug delivery system and it has special importance in the case of a payload such as DNR, which has a very narrow therapeutic window. One of the features of this delivery system highlighted by the present work is the possibility of administering mixtures of pSi particles to provide different release rates, in order to deliver high doses at an early stage in the treatment while prolonging the duration of lower drug concentration at later stages--a ubiquitous challenge for intravitreal colloidal drug delivery systems.

DNR is a potent antiproliferative agent and even stronger than the benchmark 5-fluorouracil (5-FU).[28] The inhibitory effect varies for different cells and can be as low as 0.001 μM (0.5 ng/mL).[28] In the current study, a 3 mg dose of $pSiO_2$-CO_2H:DNR particles (Type D) yielded a final vitreous DNR concentration of 67 ng/mL and 25% of this concentration (17 ng/mL) demonstrated a significant inhibitory effect on the cultured ARPE-19 cells (22% inhibition compared with control) after a 5-day exposure. The effective concentration in vivo is not well determined because it largely depends on both concentration and duration of exposure. A sustained lower concentration may be as effective as or show a higher therapeutic effect than a short exposure to a higher concentration of the drug, such as a 2.6 μg [26] or 5 μg [27] intravitreal bolus injection. For example, it has been reported that exposure to 700 nM of DNR for 1 hour inhibits 50% of fibroblast proliferation, but cell proliferation is completely inhibited by exposure to lower concentrations (500 nM) for longer times (5 hours).[8] Machemer and colleagues reported that a single intravitreal dose of 15 nmol per eye on the 3rd day following intravitreal cell injection was not effective in preventing retinal detachment. However splitting the dose into 10 nmol and 5 nmol injected 4 hours apart was effective. This suggests that sustained drug exposure at the disease site can drive the minimum effective concentration of a drug much lower.[5] Indeed, in another in vivo study Peyman and colleagues found that sustained release (21 days) of DNR in vitreous at a concentration of 5~60 ng/mL resulted insignificant inhibition of PVR development.[29] Our previous work [10, 11] suggests that this pSi-based DNR delivery system may provide a sustained DNR level in vitreous because the DNR loaded pSi particles was seen for 2–3 months following a single intravitreal injection.

Pore size and porosity are known to be related to the degradation rate of the pSi host matrix. [13] In general, greater pore size and greater porosity leads to greater dissolution rates.[30] However, greater dissolution rate of pSi does not always translate into faster payload release. Recently Martinez and colleagues demonstrated that larger pored porous silicon particles displayed faster degradation and higher loading of quantum dots, while exhibiting the slowest release rate of the payload.[14] It seems that drug release from pSi not only depends on pore size of pSi but also depends on payloads and loading mechanisms. Our ultimate goal in developing a sustained intraocular delivery system is to keep the therapeutic drug level at the disease site for several months or longer to reduce the eye injection frequency (6 to 12 times/year) which has become a major burden for patients and health care providers.[31] In the context of covalent loading and the drug Daunorubicin, we were interested in knowing firstly if pore size change will cause substantial changes of porous silicon degradation; secondly if these changes will be translated into drug release rate changes; thirdly if observed changes in vitro will be translated into in vivo and be potentially therapeutic. Therefore, our execution of the experiments was staged so that we were allowed to optimize the next stage design according to preceding stage results. In the current study, increasing pore size from 15 to 43 nm (corresponding porosities 46% and 73%, respectively) appeared to increase the rate of particle dissolution (as measured by the appearance of free silicic acid in solution, Fig. 3). However, there was no statistically significant difference between the two smaller pore particles which had 15 and 26 nanometer pores. Hence, in our second stage of our hypothesis testing, we dropped the 26 nanometer pore particle and added

the 95 nm pore particle which is the largest pore we can make within the sizes of particles we used. In the in vitro dynamic drug release study, even larger differences in pore size (from 15 nm to 43 nm instead of to 26 nm) did not show a large difference of drug release rate in vitro (Fig. 5) or in vivo (Fig. 6). In contrast, increasing pore size from 43 nm to 95 nm (porosity 76%) led to a significant increase of drug release both in vitro (Fig. 5) and in vivo (Fig. 6). This non-linear relation between pore size increase and pSi degradation increase was also observed in vitro by Martinez and colleagues.[14] Although the same ultrasonication conditions were used to break the etched films into particles, the 95 nm pore size material fractured into significantly smaller particles than the formulations with the smaller pore dimensions (Table 2). This can be explained by the decrease in wall thickness as the pore size enlarges, which may facilitate the fracture of the $pSiO_2$ matrix during ultrasonication, and a more rapid dissolution profile when tested in vitro and in vivo. We hypothesize that a similar situation will develop in the rabbit eye in which $pSiO_2$ matrix degrades over time but $pSiO_2$ particles with 95 nm pore may break into numerous smaller particles due to pore wall collapsing, resulting in much larger total surface area. All of these aspects may contribute to the observed acceleration or non-linearity in particle degradation and drug release from the $pSiO_2$-CO_2H:DNR particles with different pore sizes.

Comparing in vitro and in vivo daunorubicin release, it seems that the results from the in vitro dynamic release are in agreement with the results from the in vivo study even though in vivo daunorubicin from the largest pore particles at week 2 was higher than that in vitro (32 ng/mL vs. 16 ng/mL).The in vitro dynamic dissolution chamber used a 1.5 mL volume similar to rabbit vitreous volume [22] and a 1 μL/min infusion rate similar to rabbit vitreous fluid turnover.[32] The observed faster drug release from the 95 nm pore particles in vivo may be contributed to the breakup of the particle into multiple smaller pieces, which may more easily happen in a moving rabbit vitreous than in a fixed diffusion chamber. In addition, the vitreous may erode the pSi particles quicker than the PBS in the dissolution chambers.

The ability to engineer pore sizes by controlling the electrochemical etching parameters is a unique feature of the pSi system.[33] Some of the key properties of a pSi film such as porosity and pore size are mainly determined by the etching current density and the composition of the etching solution.[15] Typically, larger current density generates larger pores, which in combination with the etching solution composition enables a wide range of possibilities to tune the pSi nanostructure. These means of regulation allow for a generation of pSi particles with tailored pore sizes and volumes that enhance both the control of drug release and the efficiency of drug loading. Many current drug delivery materials are dense and can only deliver a small mass percentage of drugs. With a free volume typically between 50% and 70%, the pSi system offers a clear advantage over non porous or less tunable drug delivery systems.[30] In the current study, pore size and porosity were varied from 15 nm to 95 nm and 50% to 76%, respectively, resulting in DNR concentrations in rabbit vitreous at 2 weeks ranging from 1.05 ng/mL to 66.52 ng/mL.

In conclusion, the current study is a proof of concept study which demonstrates a feasible sustained intravitreal DNR delivery system that is efficient and tunable by engineering the pore size of the porous silicon. This $pSiO_2$ intravitreal drug release system allows regulation of the drug level in the eye by a factor of 60. Although the non-linear relationship between different particle's degradation and payload release warrants further exploration, the current study results suggest that a formulation containing a mixture of pSi particles with different pore sizes could be used to optimize the drug release profile for a range of eye diseases and therapeutic molecules.

Acknowledgments

A.N. acknowledges the Foundation Alfonso Martin Escudero for a postdoctoral fellowship.

Financial support: This study was supported by the National Institutes of Health under grant number NIH EY020617

References

1. Berger W, Kloeckener-Gruissem B, Neidhardt J. The molecular basis of human retinal and vitreoretinal diseases. Prog Retin Eye Res. 2010; 29:335–375. [PubMed: 20362068]
2. Cheng L, Hostetler K, Valiaeva N, Tammewar A, Freeman WR, Beadle J, Bartsch DU, Aldern K, Falkenstein I. Intravitreal crystalline drug delivery for intraocular proliferation diseases. Invest Ophthalmol Vis Sci. 2010; 51:474–481. [PubMed: 19696179]
3. Peyman GA, Schulman J. Proliferative vitreoretinopathy and chemotherapeutic agents. Surv Ophthalmol. 1985; 29:434–442. [PubMed: 3892742]
4. Shinohara K, Tanaka M, Sakuma T, Kobayashi Y. Efficacy of daunorubicin encapsulated in liposome for the treatment of proliferative vitreoretinopathy. Ophthalmic Surg Lasers Imaging. 2003; 34:299–305. [PubMed: 12875458]
5. Khawly JA, Saloupis P, Hatchell DL, Machemer R. Daunorubicin treatment in a refined experimental model of proliferative vitreoretinopathy. Graefes Arch Clin Exp Ophthalmol. 1991; 229:464–467. [PubMed: 1937080]
6. Wiedemann P, Hilgers RD, Bauer P, Heimann K. Adjunctive daunorubicin in the treatment of proliferative vitreoretinopathy: results of a multicenter clinical trial. Daunomycin Study Group. Am J Ophthalmol. 1998; 126:550–559. [PubMed: 9780100]
7. Kumar A, Nainiwal S, Choudhary I, Tewari HK, Verma LK. Role of daunorubicin in inhibiting proliferative vitreoretinopathy after retinal detachment surgery. Clin Experiment Ophthalmol. 2002; 30:348–351. [PubMed: 12213159]
8. Wiedemann P, Sorgente N, Bekhor C, Patterson R, Tran T, Ryan SJ. Daunomycin in the treatment of experimental proliferative vitreoretinopathy. Effective doses in vitro and in vivo. Invest Ophthalmol Vis Sci. 1985; 26:719–725. [PubMed: 3997421]
9. Cheng L, Anglin E, Cunin F, Kim D, Sailor MJ, Falkenstein I, Tammewar A, Freeman WR. Intravitreal properties of porous silicon photonic crystals: a potential self-reporting intraocular drug-delivery vehicle. Br J Ophthalmol. 2008; 92:705–711. [PubMed: 18441177]
10. Chhablani J, Nieto A, Hou H, Wu EC, Freeman WR, Sailor MJ, Cheng L. Oxidized porous silicon particles covalently grafted with daunorubicin as a sustained intraocular drug delivery system. Invest Ophthalmol Vis Sci. 2013
11. Hartmann KI, Nieto A, Wu EC, Freeman WR, Kim JS, Chhablani J, Sailor MJ, Cheng L. Hydrosilylated porous silicon particles function as an intravitreal drug delivery system for daunorubicin. J Ocul Pharmacol Ther. 2013; 29:493–500. [PubMed: 23448595]
12. Nieto A, Hou H, Sailor MJ, Freeman WR, Cheng L. Ocular silicon distribution and clearance following intravitreal injection of porous silicon microparticles. Experimental Eye Research. 2013; 116:161–168. [PubMed: 24036388]
13. Anderson SHC, Elliott H, Wallis DJ, Canham LT, Powell JJ. Dissolution of different forms of partially porous silicon wafers under simulated physiological conditions. phys. stat. sol. (a). 2003; 197:331–335.
14. Martinez JO, Chiappini C, Ziemys A, Faust AM, Kojic M, Liu X, Ferrari M, Tasciotti E. Engineering multi-stage nanovectors for controlled degradation and tunable release kinetics. Biomaterials. 2013; 34:8469–8477. [PubMed: 23911070]
15. Sailor, MJ. Characterization, and Applications. Wiley-VCH; 2012. Porous Silicon in Practice: Preparation.
16. Wu EC, Andrew JS, Buyanin A, Kinsella JM, Sailor MJ. Suitability of porous silicon microparticles for the long-term delivery of redox-active therapeutics. Chem Commun (Camb). 2011; 47:5699–5701. [PubMed: 21503283]

17. Wu EC, Park JH, Park J, Segal E, Cunin F, Sailor MJ. Oxidation-triggered release of fluorescent molecules or drugs from mesoporous Si microparticles. ACS Nano. 2008; 2:2401–2409. [PubMed: 19206408]
18. Pacholski C, Sartor M, Sailor MJ, Cunin F, Miskelly GM. Bio sensing using porous silicon double-layer interferometers: reflective interferometric Fourier transform spectroscopy. J Am Chem Soc. 2005; 127:11636–11645. [PubMed: 16104739]
19. Gregg SJS, KSW. Adsorption Surface Area and Porosity. 2nd ed.. London: Academic Press Inc.; 1982.
20. Brunauer S EP, Teller E. Adsorption of gases in multimolecular layers. J Am Chem Soc. 1938; 60:309–319.
21. Kruk M, Jaroniec M, Sayari A. Relations between Pore Structure Parameters and Their Implications for Characterization of MCM-41 Using Gas Adsorption and X-ray Diffraction. Chem Mater. 1999; 11:492–500.
22. Kim JS, Beadle JR, Freeman WR, Hostetler KY, Hartmann K, Valiaeva N, Kozak I, Conner L, Trahan J, Aldern KA, Cheng L. A novel cytarabine crystalline lipid prodrug: hexadecyloxypropyl cytarabine 3',5'-cyclic monophosphate for proliferative vitreoretinopathy. Molecular vision. 2012; 18:1907–1917. [PubMed: 22876115]
23. Cheng LY, Hostetler KY, Gardner MF, Avila CP, Bergeron-Lynn G, Severson GM, Freeman WR. Intravitreal pharmacokinetics in rabbits of the foscarnet lipid prodrug: 1-O-octadecyl-sn-glycerol-3-phosphonoformate (ODG-PFA). Curr Eye Res. 1999; 18:161–167. [PubMed: 10342370]
24. Bartz-Schmidt U, Szurman P, Wong D, Kirchhof B. New developments in retinal detachment surgery. Ophthalmologe. 2008; 105:27–36. [PubMed: 18210123]
25. Scheer S, Morel C, Touzeau O, Sahel JA, Laroche L. Pharmacological adjuvants for surgical treatment of proliferative vitreoretinopathy. J Fr Ophtalmol. 2004; 27:1051–1059. [PubMed: 15557870]
26. Wiedemann P, Kirmani M, Santana M, Sorgente N, Ryan SJ. Control of experimental massive periretinal proliferation by daunomycin: dose-response relation. Graefes Arch Clin Exp Ophthalmol. 1983; 220:233–235. [PubMed: 6629017]
27. Santana M, Wiedemann P, Kirmani M, Minckler DS, Patterson R, Sorgente N, Ryan SJ. Daunomycin in the treatment of experimental proliferative vitreoretinopathy: retinal toxicity of intravitreal daunomycin in the rabbit. Graefes Arch Clin Exp Ophthalmol. 1984; 221:210–213. [PubMed: 6489768]
28. Hou J, Li Y, Zhou Z, Valiaeva N, Beadle JR, Hostetler K, Freeman WR, Hu DN, Chen H, Cheng L. Antiproliferative property of hexadecyloxypropyl 9-[2-(phosphonomethoxy) ethyl] guanine (HDP-PMEG) for unwanted ocular proliferation. Molecular vision. 2011; 17:627–637. [PubMed: 21386925]
29. Rahimy MH, Peyman GA, Fernandes ML, el-Sayed SH, Luo Q, Borhani H. Effects of an intravitreal daunomycin implant on experimental proliferative vitreoretinopathy: simultaneous pharmacokinetic and pharmacodynamic evaluations. J Ocul Pharmacol. 1994; 10:561–570. [PubMed: 7836865]
30. Anglin EJ, Cheng L, Freeman WR, Sailor MJ. Porous silicon in drug delivery devices and materials. Adv Drug Deliv Rev. 2008; 60:1266–1277. [PubMed: 18508154]
31. Regillo CD, Brown DM, Abraham P, Yue H, Ianchulev T, Schneider S, Shams N. Randomized, double-masked, sham-controlled trial of ranibizumab for neovascular age-related macular degeneration: PIER Study year 1. American journal of ophthalmology. 2008; 145:239–248. [PubMed: 18222192]
32. Davson H, Luck CP. Chemistry and rate of turnover of the ocular fluids of the bush baby (Galago crassicaudatus Agisymbanus). J Physiol. 1959; 145:433–439. [PubMed: 13642310]
33. Zhang G. Porous Silicon: Morphology and Formation Mechanisms. Modern Aspects of Electrochemistry. 2006; 39:65–133.

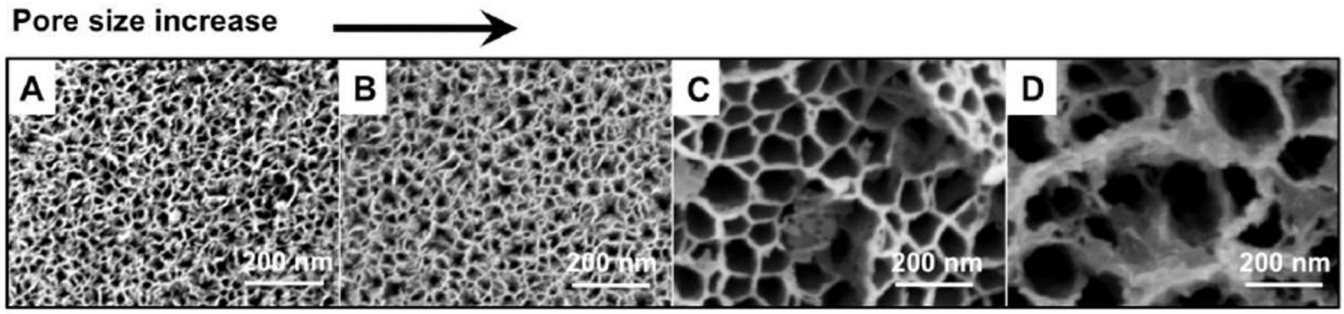

Figure 1.
Scanning electron microscope images of $pSiO_2$ particles A–D, showing a close-up view of the pores. From the images, it is clear how the etching parameters (Table 1) influence particle pore size. The same magnification was noted by scale bars for all four images.

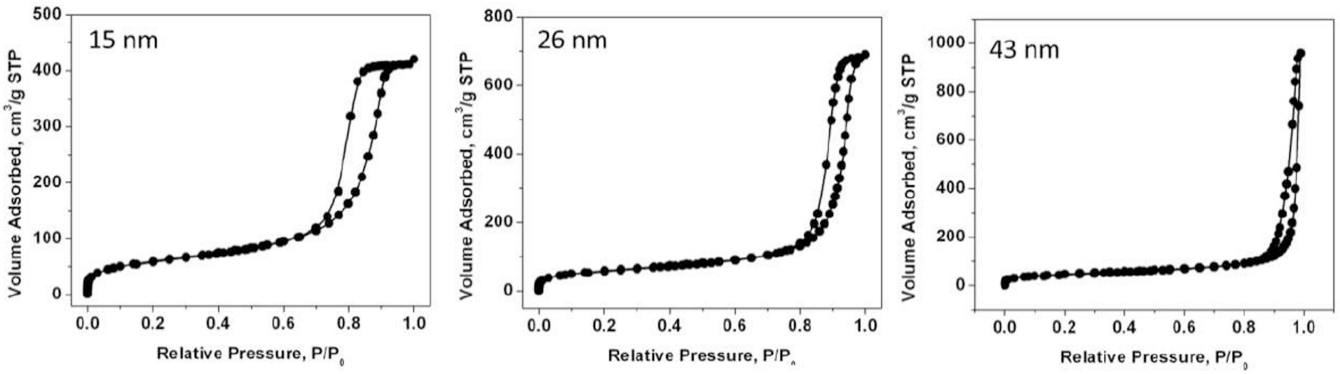

Figure 2.
Nitrogen adsorption/desorption isotherm of particle A–C.

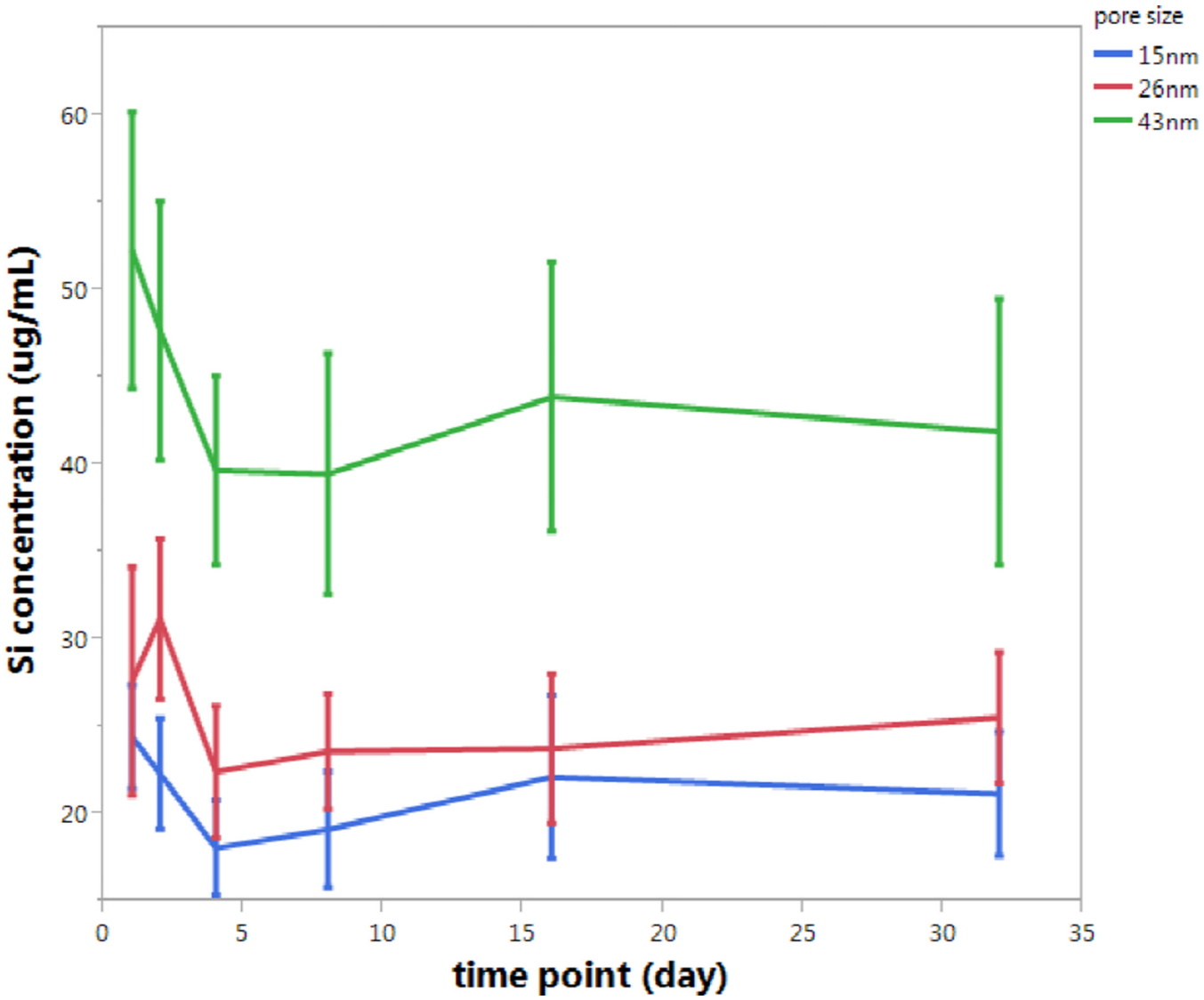

Figure 3.

Steady state concentration of soluble silicon (μg/mL) released over time during in vitro degradation of three different $pSiO_2$ microparticle formulations, containing average pore diameters of 15 nm (blue trace at the bottom, particle type A), 26 nm (red trace in the middle, particle type B) and 43 nm (green trace at the top, particle type C). Each error bar is constructed using 1 standard deviation from the mean. The data was normalized using the initial weight of the starting porous silicon particles used.

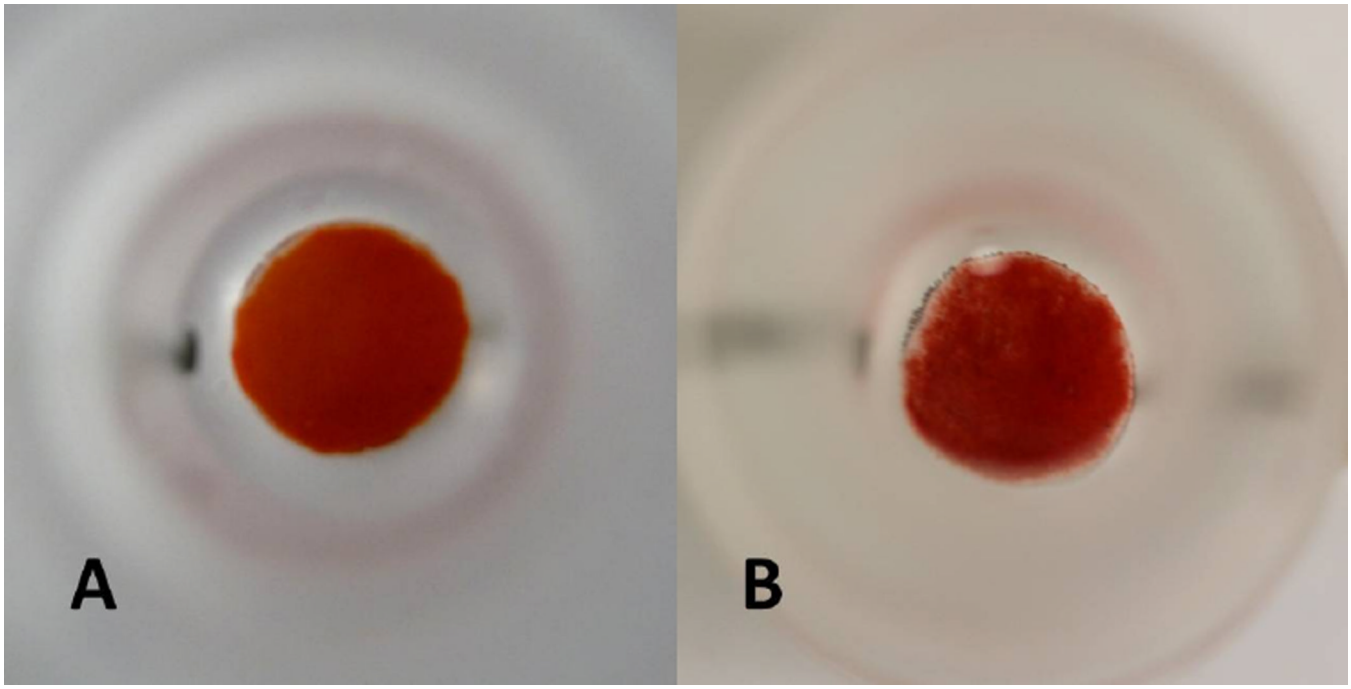

Figure 4.

Top-view of the in vitro release chamber loaded with $pSiO_2$-CO_2H:DNR particle type D: at the beginning of the in vitro release showing thicker layer of $pSiO_2$-CO_2H:DNR particle (A); at day 60 of in vitro release showing significantly thinner layer of $pSiO_2$-CO_2H:DNR particle (B).

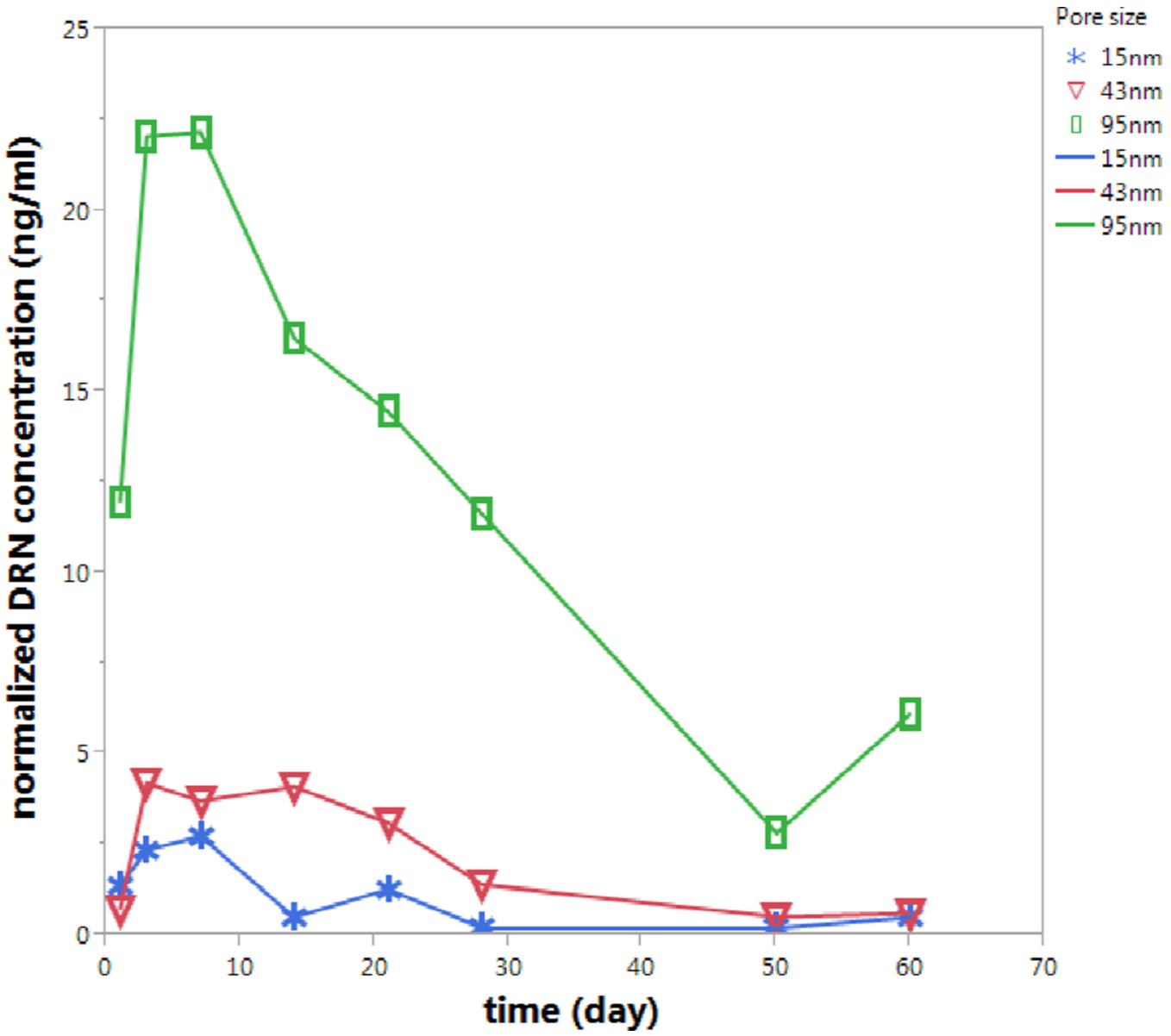

Figure 5.

DNR concentration detected by LC-MS/MS in the dynamic in vitro release apparatus. A burst release is observed at day 1–3. After wards, DNR release was sustained until the end of the 60-day observation period. Compared to particles A (blue trace, bottom) and C (red trace, middle), particle D (green trace, top) showed the largest drug level released at each time point. The data was normalized using the initial drug amount in the starting porous silicon particles used.

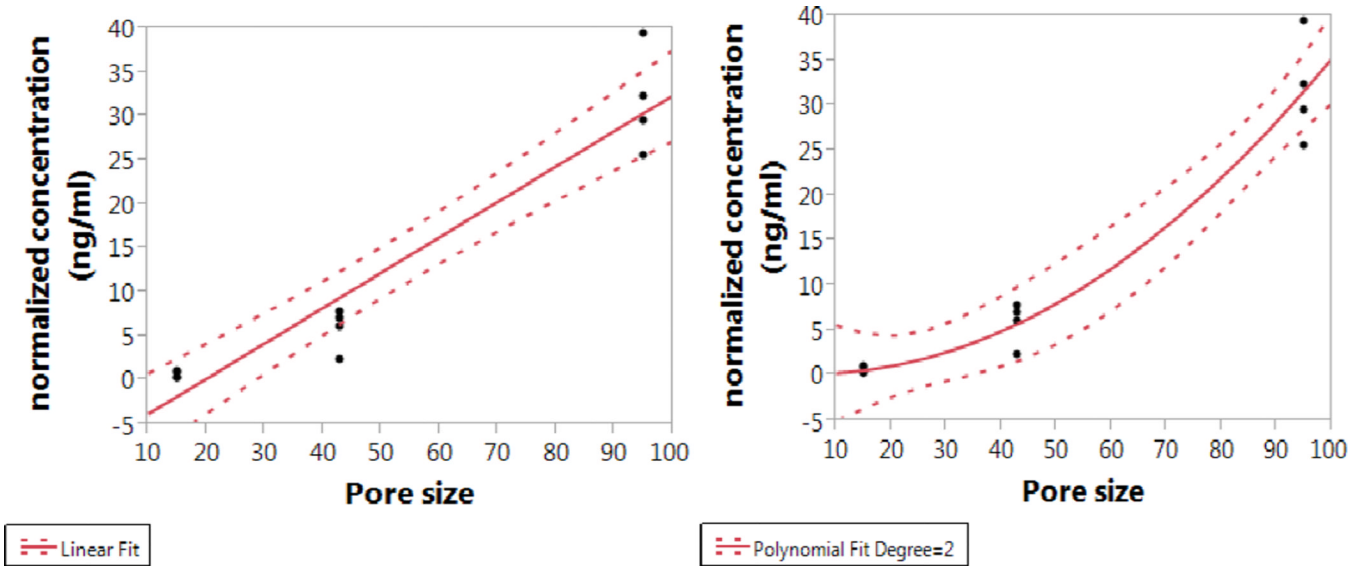

Figure 6.

Correlation of particles pore size and DNR concentrations in rabbit vitreous. For the linear fit (left), the equation is: normalized concentration (ng/ml) = −7.901656 + 0.4034276* Pore size; for the quadratic fit (right), the equation is: normalized concentration (ng/ml) = −9.888958 + 0.3585216* Pore size + 0.0038934* (Pore size-51)^2.

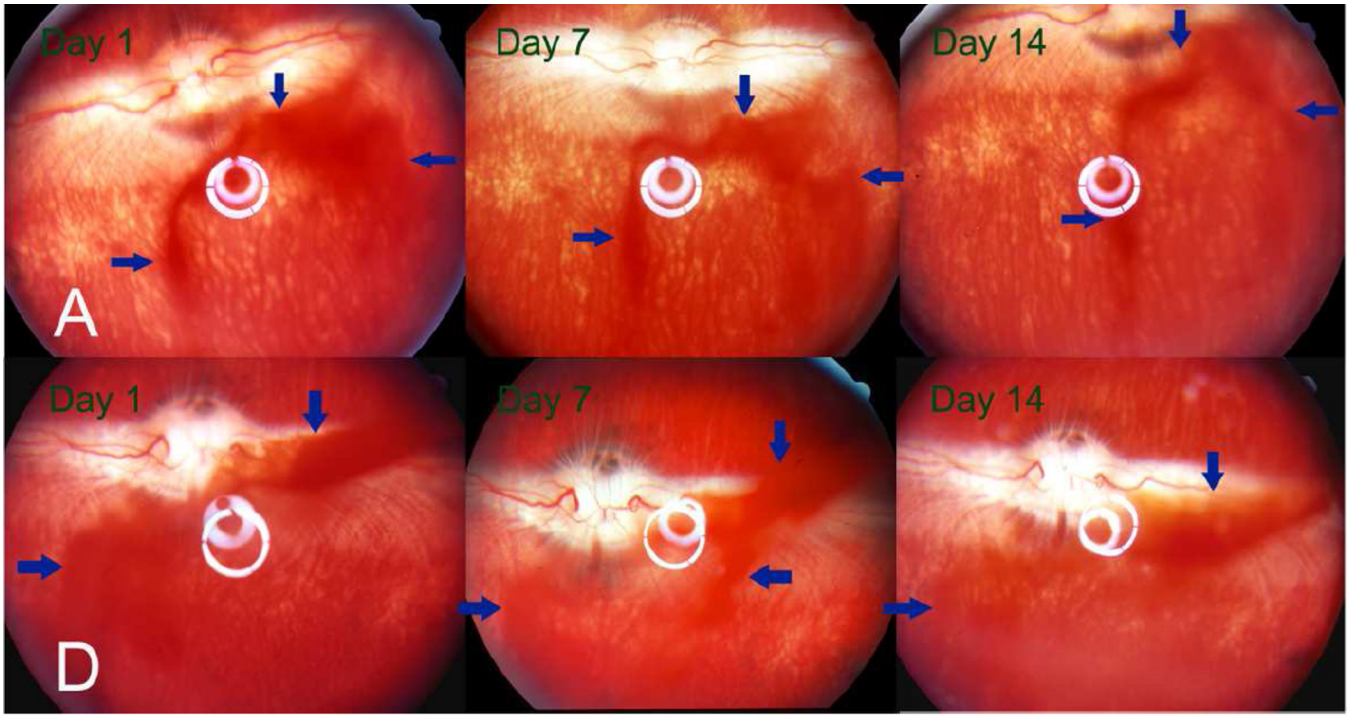

Figure 7.

Fund us images of the rabbits' eyes at observation time points 1, 7 and 14 days after injection of 3 mg particle A (upper panel) or particle D (lower panel) into the right eye of the rabbits. The DNR-loaded particles appeared reddish (arrows) due to the red color of the drug. The quantity of particles in the vitreous appeared to have decreased in both groups at 2 weeks after injection. The vitreous, retina, and optic nerve head appeared normal.

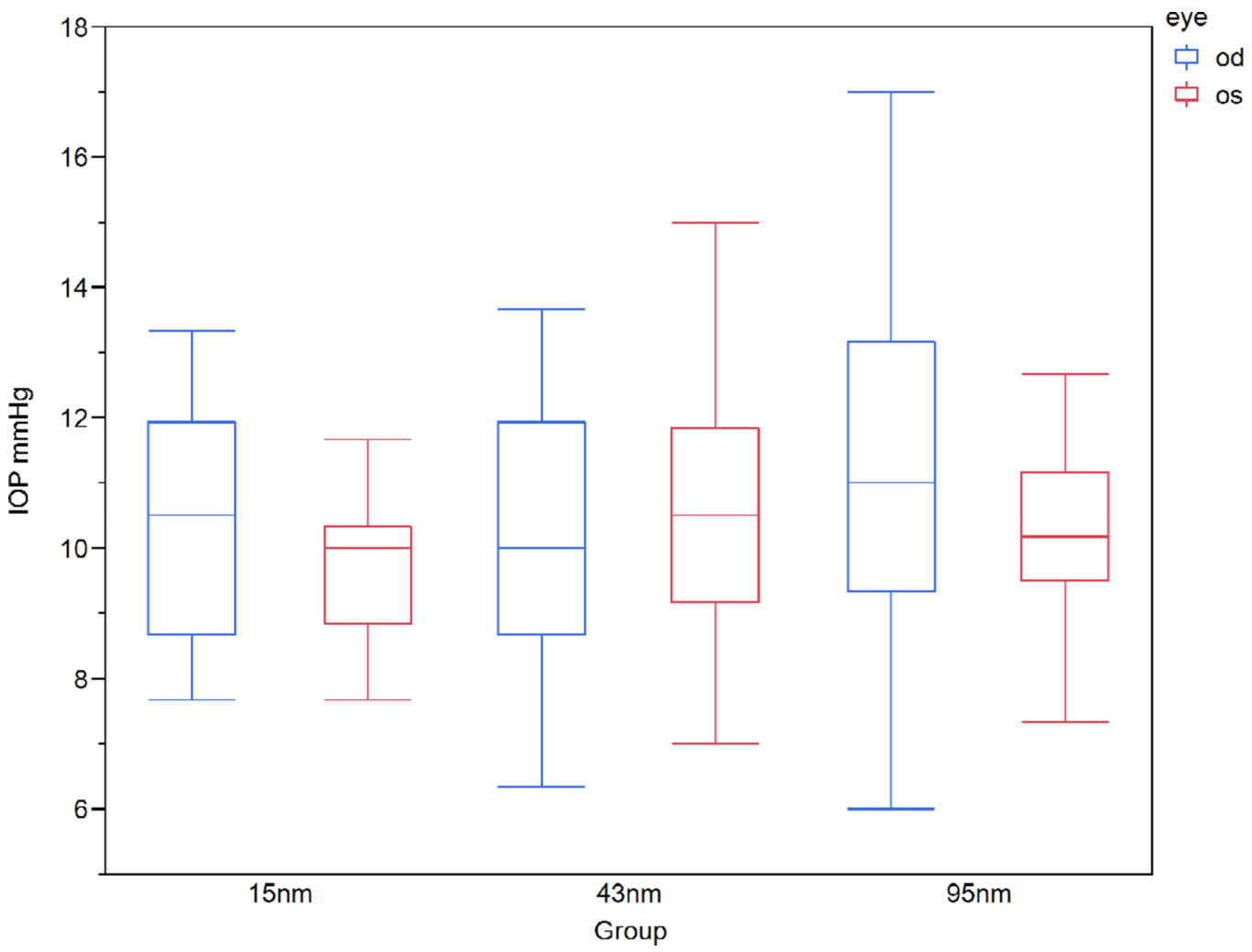

Figure 8.
Intraocular pressure (IOP) of the injected eyes and their fellow eyes stratified by particle size. No significant differences were noted between eyes or between groups.

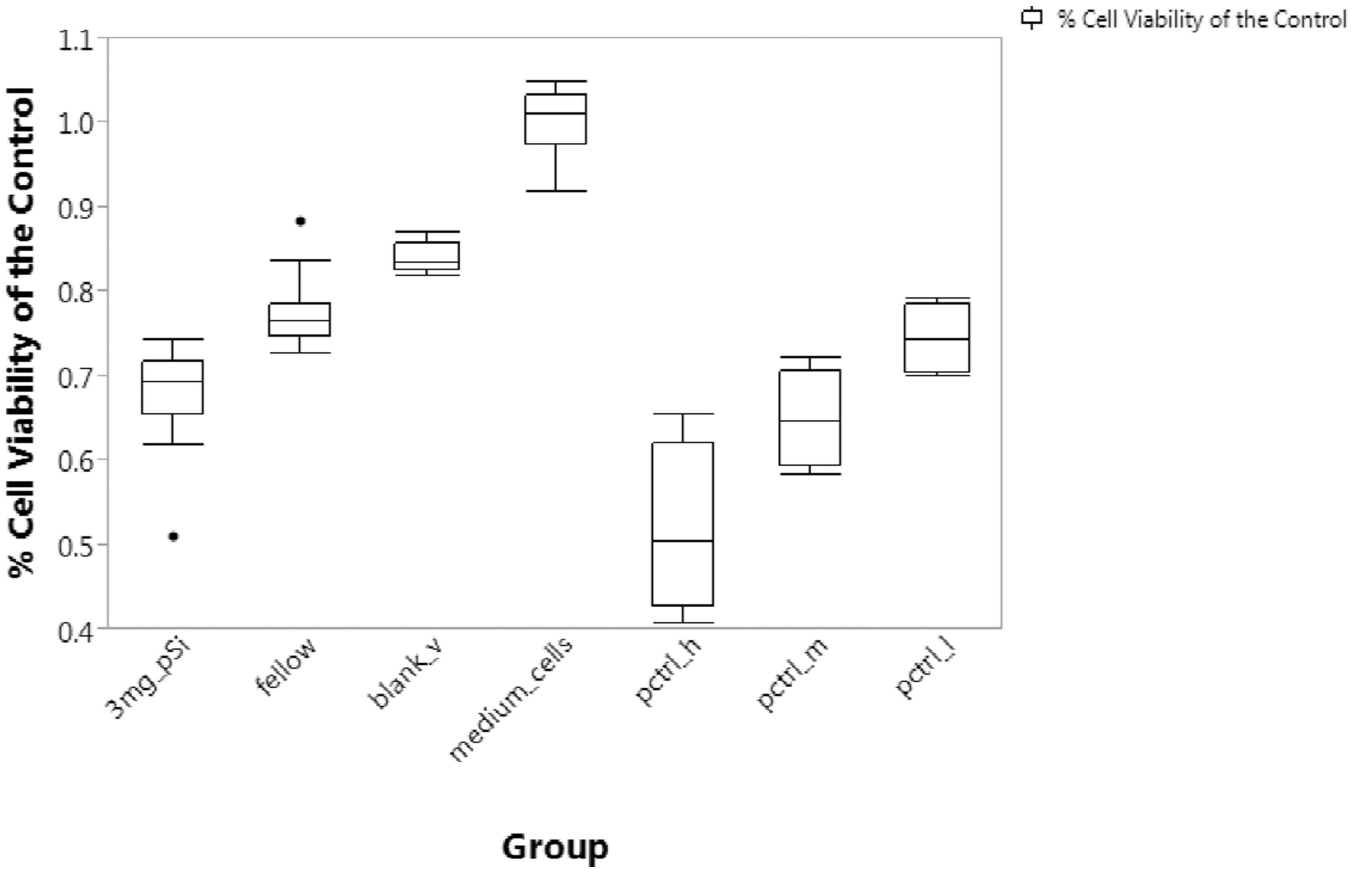

Figure 9.

Result of RPE cells proliferation assay. 3 mg_pSi: the cells were treated with a mixture 25% (by volume) of vitreous supernatant from the eyes injected with 3 mg particle D and 75% culture medium; fellow: the cells were treated with a mixture of 25% of vitreous supernatant from the fellow control eyes and 75% culture medium; blank_v: the cells were treated with a mixture 25% of normal rabbit vitreous supernatant and 75% culture medium; pctrl_m: (positive control, middle dose) cells were treated with a 100 uL aliquot of DNR of concentration 48 ng/mL, equivalent to the concentration of DNR found in the eyes 2 weeks after injection of 3 mg of particle type D. pctrl_h (positive control, high dose) and pctrl_l (positive control, low dose): DNR introduced to cells was 3.2-fold (half-log) higher or 3.2-fold lower than pctrl_m, respectively; medium cells: 100% culture medium and RPE cells as a control to calculate cell viability for the other groups.

Table 1

Parameters of pSi microparticles synthesis

Particle	Etch current density (mA/cm^2)	Etching solution (48% HF: Ethanol)	Etch duration (sec)	Lift-off current density (mA/cm^2)	Lift-off duration (sec)
A	90.2	3:1	300	6.2	120
B	300	3:1	120	6.2	120
C	60	1:1	480	6.2	120
D	70	1:1	400	6.2	120

HF: hydrofluoric acid
sec: seconds

Table 2

Texture properties and drug loading efficiency of $pSiO_2$-CO_2H:DNR particles

Particle	Particle size, μm			Porosity, %	Pore size, nm (SEM)[a]	S_{BET}, m^2/g	D_p, nm (BJH)	V_T, cm^3/g	Drug loading, μg/mg
	Width	Length	Thickness						
A	31±7	46±10	17±2	50±2	15±2	209±4	12	0.61	75±5
B	27±6	40±10	17±2	60±3	26±5	216±1	21	1.02	N/A[c]
C	23±4	37±6	13±2	73±3	43±7	168±1	45	1.44	71±5
D	15±2	20±5	13±1	76±3	95±17	154±2	45[b]	1.84	80±6

BET: Brunauer-Emmett-Teller method

BJH: Barrett-Joyner-Halenda method

S_{BET}: specific surface area

V_T: total pore volume at relative pressure (P/P_0) equal to 0.99

D_p: pore diameter calculated from the adsorption branch of the isotherm by the BJH method

[a] Pore size calculated from scanning electron microscope (SEM) images

[b] Pore size in particle D is beyond the mesopore range (2–50 nm), thus beyond the detection limit for this sorption technique

[c] Drug loading studies were not performed on this particle type

Table 3

Connecting Letters Report for Inhibition Assay on ARPE-19 Cells

Sample						Mean OD value
medium_cells	A					2.7708750
blank_v		B				2.3259833
fellow			C			2.1435313
pctrl_l			C	D		2.0601250
3 mg_pSi				D		1.8789188
pctrl_m				D		1.7958000
pctrl_h					E	1.4331250

Samples not connected by the same letter are significantly different. Comparisons for all pairs using Tukey-KRAMER HSD, α=0.05. Samples medium_cells, blank_v, fellow, pctrl_l, 3 mg_pSi, pctrl_m, pctrl_h, as defined in Figure 9 caption.